Communication

Initial Example of a Triangular Single-Molecule Magnet from Ligand-Induced Structural Distortion of a [Mn^{III}O] Complex

Theocharis C. Stamatatos, Dolos Foguet-Albiol, Constantinos C. Stoumpos, Catherine P. Raptopoulou, Aris Terzis, Wolfang Wernsdorfer, Spyros P. Perlepes, and George Christou

J. Am. Chem. Soc., **2005**, 127 (44), 15380-15381• DOI: 10.1021/ja0558138 • Publication Date (Web): 18 October 2005

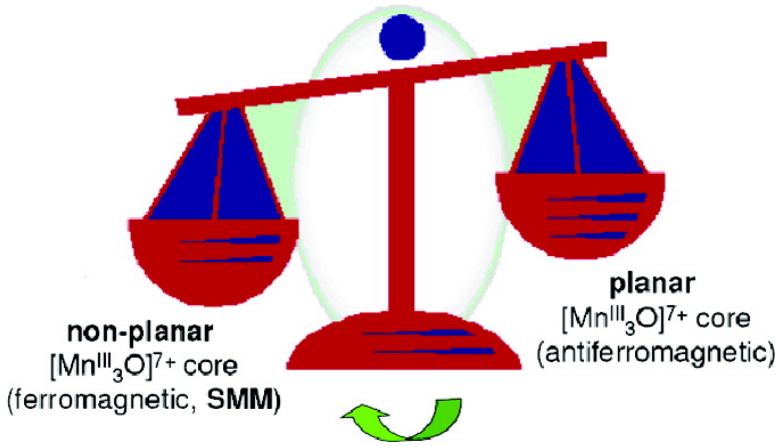

More About This Article

Additional resources and features associated with this article are available within the HTML version:

- Supporting Information
- Links to the 23 articles that cite this article, as of the time of this article download
- Access to high resolution figures
- Links to articles and content related to this article
- Copyright permission to reproduce figures and/or text from this article

View the Full Text HTML

J|A|C|S
COMMUNICATIONS

Published on Web 10/18/2005

Initial Example of a Triangular Single-Molecule Magnet from Ligand-Induced Structural Distortion of a $[Mn^{III}_3O]^{7+}$ Complex

Theocharis C. Stamatatos,[†] Dolos Foguet-Albiol,[‡] Constantinos C. Stoumpos,[†] Catherine P. Raptopoulou,[§] Aris Terzis,[§] Wolfang Wernsdorfer,[#] Spyros P. Perlepes,*[,†] and George Christou*[,‡]

Department of Chemistry, University of Patras, 26504 Patras, Greece, Department of Chemistry, University of Florida, Gainesville, Florida 32611-7200, Institute of Materials Science, NCSR "Demokritos", 15310 Aghia Paraskevi Attikis, Greece, and Laboratoire Louis Néel-CNRS, 38042 Grenoble, Cedex 9, France

Received August 24, 2005; E-mail: christou@chem.ufl.edu; perlepes@patreas.upatras.gr

Single-molecule magnets (SMMs) are individual molecules that function as nanoscale magnetic particles.[1,2] They derive their properties from the combination of a large ground-state spin (S) and a magnetoanisotropy of the Ising-type (negative zero-field splitting parameter, D).[1] They also display quantum tunneling of magnetization (QTM)[3] and quantum phase interference,[4] properties of the microscale. SMMs of various types and metal topologies are now known, with most being Mn species. There are, however, no triangular SMMs; numerous oxide-centered triangular $[M_3O(O_2CR)_6L_3]^{n+}$ (n = 0, 1) complexes are known for many transition metals,[5a] but antiferromagnetic exchange interactions within the $[M_3O]$ core lead to small S values, and they are therefore not SMMs.[5] It is thus tempting to conclude that this common triangular $[M_3O]$ structural topology can never lead to SMMs, but we show in the present work that relatively small, ligand-imposed structural distortions can alter the sign of the exchange interactions and "switch on" the SMM property.

We have been exploring the use of 2-pyridyl oximes[6] in the synthesis of 3d metal clusters, and we can now report that methyl 2-pyridyl ketone oxime (mpkoH) has yielded a new triangular $[Mn^{III}_3O]$ product. This is very unusual in being ferromagnetically coupled with a resultant S = 6 ground-state spin and is indeed the first triangular SMM.

The reaction of $[Mn_3O(O_2CMe)_6(py)_3](ClO_4)$ (**1**) with mpkoH (3 equiv) in MeOH/MeCN (1:2 v/v) gave a dark-brown solution. This was evaporated to dryness under reduced pressure, and the residue was dissolved in CH_2Cl_2 and layered with n-hexane. After 2 days, dark-brown crystals of $[Mn_3O(O_2CMe)_3(mpko)_3](ClO_4)\cdot 3CH_2Cl_2$ (**2**·$3CH_2Cl_2$) were isolated in 80−90% yield. The structure[7] of **2**·$3CH_2Cl_2$ (Figure 1) consists of a near-equilateral Mn^{III}_3 triangle capped by μ_3-O^{2-} ion O61. Each edge is bridged by an $\eta^1{:}\eta^1{:}\mu$-$MeCO_2^-$ group and an $\eta^1{:}\eta^1{:}\eta^1{:}\mu$-$mpko^-$ group, whose pyridyl ring is bound terminally to a Mn. O61 is 0.295 Å above the Mn_3 plane. The Mn^{III} oxidation states and O^{2-} protonation level were established by bond valence sum (BVS) calculations,[8,9] charge considerations, and the presence of Mn^{III} Jahn−Teller elongation axes (O1−Mn1−O31, O11−Mn2−O51, O21−Mn3−O42). The isostructural propionate analogue was prepared in an identical manner.

Variable-temperature DC magnetic susceptibility data were collected on dried **2** in the temperature range of 5.0−300 K in an applied field of 1 kG (0.1 T). $\chi_M T$ is 13.01 $cm^3\ mol^{-1}$ K at 300 K, increasing on cooling to a maximum of 19.39 $cm^3\ mol^{-1}$ K at 30.0 K, and then decreasing to 17.41 $cm^3\ mol^{-1}$ K at 5.00 K.[9] This indicates ferromagnetic exchange interactions within **2** to give an S = 6 ground state, which is consistent with the 30.0 K value (spin-only (g = 2) value for S = 6 is 21 $cm^3\ mol^{-1}$ K). The low temperature decrease is assigned to Zeeman effects, zero-field splitting, and/or weak intermolecular interactions. The data were fit to the theoretical expression for a $3Mn^{III}$ isosceles triangle.[9,10]

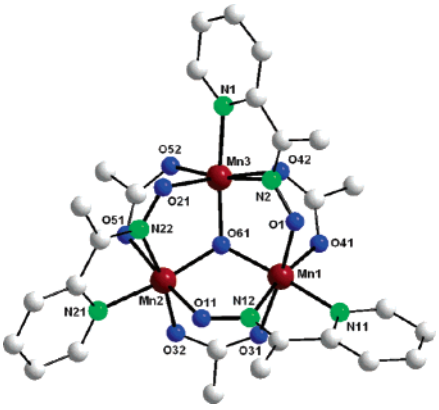

Figure 1. Molecular structure of **2**. Color code: brown, manganese; blue, oxygen; green, nitrogen; gray, carbon.

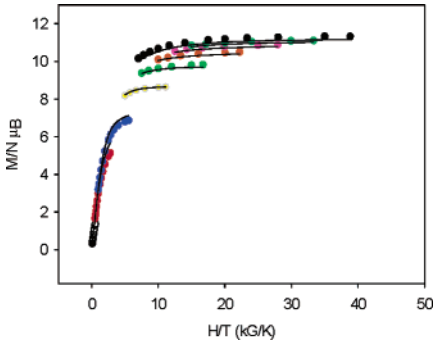

Figure 2. Plot of $M/N\mu_B$ versus H/T for complex **2** at 7 (black dot), 6 (dark green dot), 5 (magenta dot), 4 (orange dot), 3 (light green dot), 2 (yellow dot), 1 (blue dot), 0.5 (red dot), and 0.1 (open dot) tesla. The solid lines are the fit of the data.

To confirm the ground state of **2**, magnetization (M) data were collected in the 0.1−7 T and 1.8−10.0 K ranges, and these are plotted as $M/N\mu_B$ versus H/T in Figure 2. The data were fit by matrix-diagonalization to a model that assumes only the ground state is populated, includes axial zero-field splitting ($D\hat{S}_z^2$) and the Zeeman interaction, and carries out a full powder average; the spin Hamiltonian is given by eq 1, where μ_B is the Bohr magneton and μ_0 is the vacuum permeability, $\hat{S}_z$

$$H = D\hat{S}_z^{\,2} + g\mu_B\mu_0\hat{S}_z H_z \qquad (1)$$

is the easy-axis spin operator, and H_z is the applied field. The fit (solid lines in Figure 2) gave S = 6, g = 1.92, and D = −0.34 cm^{-1}.[11]

[†] University of Patras.
[‡] University of Florida.
[§] NCSR "Demokritos".
[#] Laboratoire Louis Néel-CNRS.

10.1021/ja0558138 CCC: $30.25

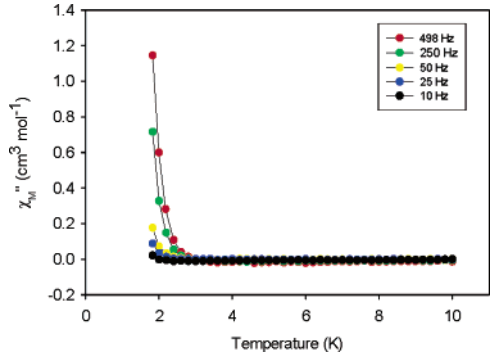

Figure 3. Plot of the out-of-phase (χ_M'') AC susceptibility signal versus temperature for a microcrystalline sample of complex **2**.

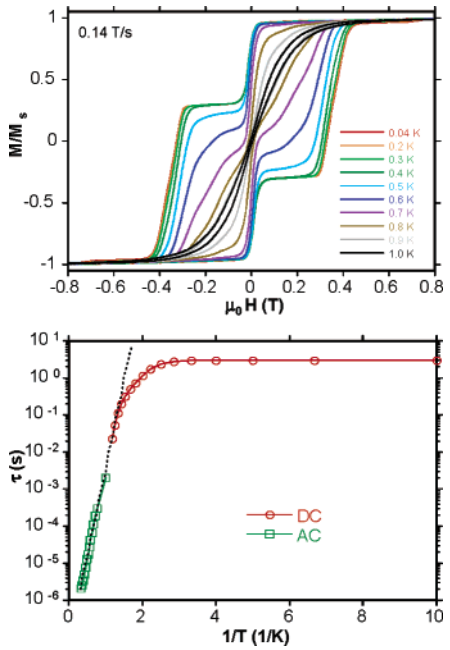

Figure 4. (Top) Magnetization versus field hysteresis loops for a single crystal of **2**·$3CH_2Cl_2$ at the indicated temperatures; *M* is normalized to its saturation value, M_S. (Bottom) Arrhenius plot constructed from AC χ_M'' versus *T* and DC magnetization decay versus time data. The dashed line is the fit of the thermally activated region to the Arrhenius equation.

Since **2** has significant *S* and *D* values, we investigated whether it is a SMM by AC susceptibility measurements in a 3.5 G AC field (Figure 3). Indeed, a frequency-dependent decrease in the in-phase ($\chi_M'T$) signal[9] and a concomitant out-of-phase (χ_M'') signal were seen at <3 K (Figure 3), indicative of the slow magnetization relaxation of SMMs. Since intermolecular interactions and phonon bottlenecks can also give such signals,[12] confirmation that **2** is a SMM was sought by magnetization versus DC field scans on single crystals of **2**·$3CH_2Cl_2$ using a micro-SQUID.[13] Hysteresis, the diagnostic property of a magnet, was observed below ~1.0 K (Figure 4, top). The loops exhibit increasing coercivity with decreasing temperature and increasing field sweep rate,[9] as expected for a SMM. The loops also display the steps indicative of QTM between M_S levels of the $S = 6$ ground state, with the temperature independent coercivity at ≤0.3 K, indicating ground state QTM, that is, only between the lowest energy $M_S = \pm 6$ levels.

AC data to lower *T* and magnetization decay versus time data were collected and used to construct Figure 4 (bottom), based on the Arrhenius relationship $\tau = \tau_0 \exp(U_{eff}/kT)$, where U_{eff} is the effective relaxation barrier, τ is the relaxation time, and *k* is the Boltzmann constant. The slope in the thermally activated region gave $U_{eff} = 10.9$ K and $\tau_0 = 5.7 \times 10^{-8}$ s. Below 0.3 K, the relaxation was temperature-independent, consistent with relaxation by ground-state QTM.

Complex **2** is thus confirmed to be a SMM, the first with a triangular topology. What now demands explanation is why **2** is ferromagnetically coupled and a SMM whereas the many previous triangular $[Mn_3O(O_2CR)_6L_3]^+$ complexes (such as **1**) are antiferromagnetically coupled and are not? We believe the answer is that **2** has its central O^{2-} ion 0.295 Å above the Mn_3 plane due to the tridentate binding of the mpko$^-$ ligand, whereas the O^{2-} ion in **1** and related species is in the Mn_3 plane, or essentially so (<0.03 Å). The central O^{2-} strongly mediates antiferromagnetic exchange via $M_{d\pi}-O_{p\pi}-M_{d\pi}$ orbital overlap, and any distortion away from planarity will thus weaken antiferromagnetic contributions to the observed exchange, J_{obs}, between two Mn atoms. Since J_{obs} is the sum of ferro- and antiferromagnetic contributions, and J_{obs} is in any case only weakly antiferromagnetic in $[Mn_3O(O_2CR)_6L_3]^+$ complexes,[5] it is reasonable that structural distortion to a nonplanar $[Mn_3O]^{7+}$ core would lead to ferromagnetic J_{obs} and a resultant $S = 6$ ground state.[14]

In conclusion, the distortion imposed on a $[Mn_3O]^{7+}$ member of the venerable class of triangular, oxide-centered $[M_3O]^{6+,7+}$ complexes by a tridentate oximate ligand switches the exchange coupling to ferromagnetic and makes **2** the initial example of a triangular SMM. This suggests that it may also be possible to modify other triangular (or other) structures with chelating and/or bridging ligands to switch on the properties of a SMM.

Acknowledgment. Th.C.S. and S.P.P. thank the Program PYTHAGORAS (Grant b.365.037) for funding. G.C. thanks the U.S.A. National Science Foundation (Grant CHE-0414155).

Supporting Information Available: Crystallographic details in CIF format, bond valence sums, and magnetism data. This material is available free of charge via the Internet at http://pubs.acs.org.

References

(1) Christou, G.; Gatteschi, D.; Hendrickson, D. N.; Sessoli, R. *MRS Bull.* **2000**, *25*, 66−71 and references therein.
(2) (a) Sessoli, R.; Gatteschi, D.; Caneschi, A.; Novak, M. A. *Nature* **1993**, *365*, 141−143. (b) Sessoli, R.; Tsai, H. L.; Schake, A. R.; Wang, S.; Vincent, J. B.; Folting, K.; Gatteschi, D.; Christou, G.; Hendrickson, D. N. *J. Am. Chem. Soc.* **1993**, *115*, 1804−1816.
(3) Friedman, J. R.; Sarachik, M. P.; Tejada, J.; Ziolo, R. *Phys. Rev. Lett.* **1996**, *76*, 3830.
(4) Wernsdorfer, W.; Sessoli, R. *Science* **1999**, *284*, 133−135.
(5) (a) Vincent, J. B.; Chang, H.-R.; Folting, K.; Huffman, J. C.; Christou, G.; Hendrickson, D. N. *J. Am. Chem. Soc.* **1987**, *109*, 5703−5711 and references therein. (b) Jones, L. F.; Rajaraman, G.; Brockman, J.; Murugesu, M.; Sanudo, C. E.; Raftery, J.; Teat, S. J.; Wernsdorfer, W.; Christou, G.; Brechin, E. K.; Collison, D. *Chem.—Eur. J.* **2004**, *10*, 5180.
(6) (a) For a review, see: Milios, C. J.; Stamatatos, Th. C.; Perlepes, S. P. *Polyhedron*, in press, and references therein. (b) Weyhermueller, T.; Wagner, R.; Khanra, S.; Chaudhuri, P. *Dalton Trans.* **2005**, 2539.
(7) Anal. Calcd (found) for dried **2** (solvent-free): C 37.59 (37.32), H 3.50 (3.49), N 9.74 (9.54). Crystal data for **2**·$3CH_2Cl_2$: $C_{33}H_{36}N_6O_{14}Cl_7Mn_3$, 1117.54 g mol^{-1}, monoclinic $P2_1/c$, $a = 12.986(5)$ Å, $b = 14.978(6)$ Å, $c = 23.150(10)$ Å, $\beta = 93.82(2)°$, $Z = 4$, $V = 4493(3)$ Å^3, $d_{calcd} = 1.492$ g cm^{-3}, $T = 293(2)$ K. Final $R1 = 6.96$ and $wR2 = 19.36\%$.
(8) (a) Liu, W.; Thorp, H. H. *Inorg. Chem.* **1993**, *32*, 4102−4105. (b) BVS for the Mn^{3+} and O^{2-} ions were 3.03−3.12 and 2.08, respectively.
(9) See Supporting Information.
(10) The fit gave $J = +14.1$ cm^{-1}, $J' = +3.8$ cm^{-1}, $g = 1.91$, and 0.9% paramagnetic impurity term; the TIP was held constant at 600×10^{-6} cm^3 mol^{-1}. Equilateral $[M_3O]$ triangles undergo the magnetic Jahn−Teller distortion, resulting in an isosceles (2*J*) situation. See: Cannon, R. D.; Jayasooriya, U. A.; Wu, R.; arapKoske, S. K.; Stride, J. A.; Nielsen, O. F.; White, R. P.; Kearley, G. J.; Summerfields, D. *J. Am. Chem. Soc.* **1994**, *116*, 11869−11874 and references therein.
(11) The fit for the propionate analogue of **2** gave $S = 6$, $g = 1.93$, and $D = -0.34$ cm^{-1}; this complex gives the same ac susceptibility data as **2**.
(12) Chakov, N. E.; Wernsdorfer, W.; Abboud, K. A.; Christou, G. *Inorg. Chem.* **2004**, *43*, 5919−5930.
(13) Wernsdorfer, W. *Adv. Chem. Phys.* **2001**, *118*, 99−190.
(14) The *D* value will also be affected by this distortion, as the single-ion anisotropy axes are tilted. Details will be provided in the full paper.

JA0558138